# $^1$H NMR Spectroscopic Studies of Calcium-Binding Proteins. 1. Stepwise Proteolysis of the C-Terminal α-Helix of a Helix–Loop–Helix Metal-Binding Domain†

David C. Corson, Thomas C. Williams,* Lewis E. Kay, and Brian D. Sykes
*Medical Research Council of Canada Group in Protein Structure and Function and Department of Biochemistry, University of Alberta, Edmonton, Alberta, Canada T6G 2H7*

*Received July 18, 1985*

ABSTRACT: A series of modified parvalbumins, differing only in length of α-helix F at the C-terminus, was prepared by carboxypeptidase-mediated digestions of the β-lineage parvalbumin (p*I* = 4.25) from carp (N; 108 residues). Removal of Ala-108 to form the N-1 derivative (des-Ala$^{108}$-parvalbumin) or removal of Ala-108 and Lys-107 to form the N-2 derivative (des-Ala$^{108}$,Lys$^{107}$-parvalbumin) only slightly alters the protein's ability to chelate Ca(II) or lanthanides(III). Analysis of the kinetics of their Yb(III) off-rates by optical stopped-flow techniques, determination of their Lu(III)-binding constants by high-resolution $^1$H NMR methods, and inspection of their solution structures by Yb(III)-shifted $^1$H NMR techniques indicate N-1 and N-2 are very similar to N (0.1–0.2 M KCl; pH 6–7; 23–55 °C). However, removal of the next one or two residues, Val-106 or Val-106/Leu-105, to generate the N-3 and N-4 derivatives severely alters the metal ion binding characteristics of the protein. Although two Yb(III) off-rates are observed for N-3, both are faster than that for the unmodified protein: $k_{CD}$ by a factor of 2 and $k_{EF}$ by a factor of 2200. Removal of Ala-104 and Ala-104/Thr-103 to give a mixture of N-5 and N-6 derivatives eliminates the slow-release site altogether, the single observable $k_{off}$ being 20–30 times faster than release of Yb(III) from the CD site of native parvalbumin. Removal of the C-terminal α-helix by digestion through Phe-102 to give N-7 destabilizes the entire protein structure as judged both by the random-coil appearance of its $^1$H NMR spectrum and by its aberrant kinetics. Although one abnormally fast $k_{off}$ is still observed at micromolar concentrations, Ln(III) chelation tends to precipitate N-7 at higher parvalbumin concentrations (1–3 mM). In contrast to the critical instability of the N-3 through N-7 derivatives, the remarkable stability of the N-1 and N-2 forms of carp parvalbumin may be attributed to the maintainance of two key structural features: an ion pair bond between the negatively charged C-terminal carboxyl function and the protonated $\epsilon$-$NH_3^+$ of Lys-27 and hydrophobic interactions of the inner side of helix F with residues in the protein's core.

Calmodulins, troponins C's, parvalbumins, the brain-specific S-100 proteins, and certain intestinal mucosal proteins share both marked amino acid sequence homology and the capacity to tenaciously chelate calcium(II) (Seamon & Kretsinger, 1983). X-ray crystallographic studies of the β-lineage p*I* = 4.25 isoform of carp parvalbumin (Kretsinger & Nockolds, 1973), bovine intestinal calcium-binding protein (Szebenyi et al., 1981), turkey gizzard troponin C (Herzberg & James, 1985), and chicken gizzard troponin C (Sundaralingam et al., 1985) indicate that each bound calcium(II) is associated with a discrete 30–35-residue substructure of the protein known as a helix–loop–helix domain. Sequence alignment suggests that there are four such substructures in calmodulins and troponin C's, three in parvalbumins and oncomodulin, and two in brain-specific S-100 and intestinal calcium-binding proteins (Barker et al., 1978); biochemically functional single-domain proteins do *not* exist. Oxygen-containing ligands from both backbone and side-chain positions of the loop chelate the bound metal ion; those domains whose loops lack the full requisite of 10–12 residues show diminished or no capacity to bind divalent metal ions (e.g., the N-terminal helix–loop–helix structure in cardiac troponins C's, domain I, and in parvalbumins, domain II). The functions served by the helices, however, are not well understood. In $Ca_2$ parvalbumins, for example, hydrophobic residues from all six helices of their three helix–loop–helix domains contribute to a fluid inner core, but the specific helical interactions that stabilize the metal-bound or apo forms of the protein have not yet been defined. Indeed, numerous reports suggest that the metal ion binding process itself induces the formation of amphipathic α-helix, the hydrophobic surfaces so formed being implicated as regions of potential protein–protein or protein–drug interactions (Gariépy & Hodges, 1983; Cachia et al., 1985). In order to probe the role played by the C-terminal α-helix in β-lineage parvalbumins, we have serially shortened helix F by digestion with carboxypeptidases A and B. Our results are compared to the conservation of specific residues involved in the helix–helix interactions of myoglobins and hemoglobins and to C-terminal ion pair bonds found in lysozyme and the deoxyhemoglobins.

## Experimental Procedures

### *Materials*

The p*I* = 4.25 isoform of carp (*Cyprinus carpio*) parvalbumin was isolated by the method of Haiech et al. (1979); its purity was verified by using amino acid analysis, UV[1] absorption and $^1$H NMR spectroscopy, and SDS–polyacrylamide gel electrophoresis. Bovine pancreatic carboxypeptidase A (CPase A; recrystallized) was purchased from Worthington Biochemical Corp., treated with DFP (Fraenkel-Conrat et al., 1955; Tschesche, 1977), and then stored at −12 °C; its activity, determined by the hippuryl-L-phenylalanine assay (Folk & Schirmer, 1963), was 35 units/mg. For removal of Ca(II), the enzyme preparation was dialyzed against 100 mM LiCl

† This work was supported by the Medical Research Council of Canada Group in Protein Structure and Function and the Alberta Heritage Foundation for Medical Research (equipment grant for the NT-300WB spectrometer, fellowship and research allowance to T.C.W., and summer studentships to L.E.K. and G. Sim).

0006-2960/86/0425-1817$01.50/0 

(pH 6.2) at 4 °C; aliquots (20 units) were then stored at −12 °C. CPase A prepared in this manner was stable for more than 1 year and showed neither tryptic nor chymotryptic activity as determined by standard assays (Tschesche, 1977). Porcine intestinal carboxypeptidase B (CPase B; type I; chromatographically purified) was purchased from Sigma; its activity, determined by the hippuryl-L-arginine assay (Folk et al., 1960), was 166 units/mg. The enzyme was dialyzed against 100 mM NaCl (pH 5.9) at 4 °C; aliquots (2 units) were then stored at −12 °C. EDTA–agarose (Haner et al., 1985) was a gift from Dr. E. R. Birnbaum, Chelex-100 (50–100 mesh) and $D_2O$ (99.8 mol %) were purchased from Bio-Rad Corp., and DE-52 (DEAE-cellulose) was purchased from Whatman Chemical Separation Ltd. Xylenol orange was purchased from Terochem Laboratories. KCl (puratronic grade), lutetium chloride ($LuCl_3 \cdot xH_2O$; REO purity), and ytterbium chloride ($YbCl_3 \cdot xH_2O$; REO purity) were purchased from Alpha Inorganics, Ventron Division.

*Proteolysis of Parvalbumin's F Helix*

Because the metal-bound forms of parvalbumin are not readily digested by carboxypeptidase, access to parvalbumin's C-terminal F helix was promoted by removal of Ca(II) from its native form. The preparation and proteolysis of apoparvalbumin were performed in 10 mM $(NH_4)_2CO_3$/100 mM KCl buffer for the following reasons: removal of Ca(II) by competition with EDTA-like chelators is sufficiently effective at pH 9.0, the upper $pK_a$ of ammonium carbonate; carboxypeptidase activity is relatively high at near-neutral pH, the lower $pK_a$ of ammonium carbonate being 6.5; gaseous Ca(II)-free $CO_2$ can be used to rapidly acidify (pH 6.5–7.0) ammonium carbonate solutions of apoparvalbumin; pH-adjusted solutions of ammonium carbonate are sufficiently stable throughout the time periods required for the carboxypeptidase-mediated digestions; unlike buffers such as Tris, ammonium carbonate contains no groups that would interfere with amino acid analysis of the digestion products, most of the ammonia being vaporized by the preceding heat treatment and lyophilization steps.

*Amino Acid Analyses.* The enzymatic release of parvalbumin's C-terminal amino acids was monitored by amino acid analyses of aliquots taken from the digestion reactions (see below). Each aliquot (10 nmol of parvalbumin) was added to 50 μL of 100 mM HCl containing 10 nmol of norleucine, immersed in boiling water for several minutes to deactivate CPase, and then dried at 77 °C. Samples (redissolved in 50 μL of 200 mM sodium citrate, pH 2.2) were eluted through an 8% cross-linked sulfonated polystyrene cation-exchange resin (Durram DC4A; 8-μm particle size; Durram Dionex D-500 amino-acid analyzer) with the following series of buffers: 200 mM sodium citrate (pH 3.25), 200 mM sodium citrate (pH 4.25), and 200 mM sodium citrate/900 mM NaCl (pH 7.9). Intact protein and large peptides elute from the column at the third buffer front. Because histidine is not present in the C-terminal portion of carp parvalbumin (and is, therefore, not released into solution), the inability to detect free histidine in the presence of protein is of no consequence. Standard sets of the amino acids (4 nmol each) were eluted periodically to provide reference ninhydrin peak areas.

*Apoparvalbumin.* An EDTA–agarose column (10 mL) was prewashed at 4 °C with the following series of solutions: 50 mL of 1 M NaCl, 20 mL of 10 mM HCl, and finally 10 mM $(NH_4)_2CO_3$/100 mM KCl, pH 9. Approximately 25 mg of $Ca_2$ parvalbumin was then applied to the column and eluted into an acid-cleaned polyethylene bottle. Alternatively, apoparvalbumin was prepared by a variation of the heated Chelex method (Bose & Bothner-By, 1983): at 25 °C, a slurry of Chelex-100 (1 g/5 mL of deionized $H_2O$) was washed first with 20 mL of 10 mM HCl and then equilibrated with 10 mM $(NH_4)_2CO_3$/100 mM KCl, pH 9. The treated resin was then transferred to a plastic container, approximately 25 mg of $Ca_2$ parvalbumin was added, and the mixture was heated to 60–63 °C for 45–60 min. While still hot, the apoparvalbumin solution was separated from the resin by elution through a small column. Calcium loss in these parvalbumin preparations was later verified by the drastically altered, random coil like appearance of the $^1H$ NMR spectrum of carp apoparvalbumin.

*Des-Ala$^{108}$-parvalbumin (N-1).* Carboxypeptidase A (20 units) was added to 25 mg of apoparvalbumin dissolved in 20 mL of ammonium carbonate buffer, pH 6.7. The solution was stirred gently for 20 min at 23 °C. Although CPase A is inhibited by basic C-terminal residues (Ambler, 1972), limited proteolysis of Ala-108 was ensured by saturating parvalbumin's two metal ion binding sites with Ca(II) and immersing the mixture in boiling water for 5 min to deactivate CPase A. If not used for the preparation of N-2 parvalbumin, the solution of the N-1 derivative was dialyzed extensively against deionized $H_2O$ and then lyophilized.

*Des-Ala$^{108}$,Lys$^{107}$-parvalbumin (N-2).* N-1 parvalbumin was prepared as described above with heat alone to deactivate CPase A; Ca(II) was *not* added. The solution was quickly cooled to room temperature and its pH readjusted to 6.7. Carboxypeptidase B (2 units) was then added, and the mixture was stirred for 60 min at 23 °C. Although the proteolytic activity of CPase B is specific for basic C-terminal residues, limited proteolysis of Lys-107 was ensured by $CaCl_2$ addition (5-fold excess) and heat treatment as before. Aliquots for amino acid analyses were taken *before* CPase A addition, *after* the first heat treatment, and *after* Ca(II) addition. N-2 parvalbumin was dialyzed against either 100 mM KCl or 5 mM $CaCl_2$ at pH 9.

*N-3 through N-6 Parvalbumins.* N-2 parvalbumin was prepared as described above, and as before, only heat treatment was used to deactivate CPase B; $CaCl_2$ was *not* added. After the solution was cooled to 20–24 °C, CPase A (20 units) was added, and the solution was stirred for 2–4 min. Proteolysis was arrested by Ca(II) addition and heat treatment. The cooled solution was dialyzed against 5 mM $CaCl_2$ (pH 9), centrifuged to remove precipitate, and then adjusted to pH 6. The mixture of Ca(II)-bound parvalbumin derivatives was loaded onto a DEAE-52 column (20 mL) and then equilibrated with 5 mM $CaCl_2$/15 mM HCl (adjusted to pH 6.0 with piperazine). Two overlapping linear KCl gradients (0.0–0.2 M and 0.1–1.0 M; 500 mL each) were applied in succession

[1] Abbreviations: N, uncleaved carp parvalbumin (β-lineage; p*I* = 4.25); N-1, des-Ala$^{108}$-parvalbumin; N-2, des-Ala$^{108}$,Lys$^{107}$-parvalbumin; N-3, des-Ala$^{108}$,Lys$^{107}$,Val$^{106}$-parvalbumin; N-4, des-Ala$^{108}$,Lys$^{107}$,Val$^{106}$,Leu$^{105}$-parvalbumin; N-5, des-Ala$^{108}$,Lys$^{107}$,Val$^{106}$,Leu$^{105}$,Ala$^{104}$-parvalbumin; N-6, des-Ala$^{108}$,Lys$^{107}$,Val$^{106}$,Leu$^{105}$,Ala$^{104}$,Thr$^{103}$-parvalbumin; N-7, des-Ala$^{108}$,Lys$^{107}$,Val$^{106}$,Leu$^{105}$,Ala$^{104}$,Thr$^{103}$,Phe$^{102}$-parvalbumin; CPase A, bovine pancreatic carboxypeptidase A; CPase B, porcine intestinal carboxypeptidase B; AB, helix A–loop–helix B region of parvalbumin (residues 7–34; domain II); CD, helix C–loop–helix D region of parvalbumin (residues 39–71; domain III); EF, helix E–loop–helix F region of parvalbumin (residues 78–108; domain IV); EDTA, ethylenediaminetetraacetic acid; DEAE-cellulose, diethylaminoethylcellulose; SDS, sodium dodecyl sulfate; $D_2O$, deuterium oxide; DFP, diisopropyl fluorophosphate; Pipes, 1,4-piperazinediethanesulfonic acid; Tris, tris(hydroxymethyl)aminomethane; DSS, sodium 4,4-dimethyl-4-silapentane-1-sulfonate; NMR, nuclear magnetic resonance; UV, ultraviolet; 1 (enzyme) unit, amount of enzyme that will catalyze the hydrolysis of 1 μmol of substrate/min.

to elute a series of peaks. From one such experiment, peak II (see Results) was shown by extensive CPase A digestion of the C-terminus (see below) to be predominantly a mixture of N-5 and N-6. From another such experiment, peak III appeared to be predominantly a mixture of N-3 and N-4 (see Results). An alternative method used to isolate an N-3/N-4 mixture relied upon the apparent solubility differences of the Yb(III) complexes of these intermediate derivatives. Because purified N-7 and N-5/N-6 mixtures showed a marked tendency to precipitate in the presence of excess Yb(III) (see Results), we added excess $YbCl_3$ to the product of a 2–4-min CPase A incubation mixture prepared as described above. The precipitate thus formed was removed by centrifugation; analysis of the amino acids released by renewed CPase A digestion indicated that the supernatant was predominantly a solution of N-3/N-4.

*Des-Ala*$^{108}$*,Lys*$^{107}$*,Val*$^{106}$*,Leu*$^{105}$*,Ala*$^{104}$*,Thr*$^{103}$*,Phe*$^{102}$*-parvalbumin (N-7).* Apoparvalbumin (32 mg) was prepared as described above. Carboxypeptidase A (400 units) was added, and the solution was stirred for 4 h at 37 °C. Samples for amino acid analyses were taken at 2 and at 4 h after mixing. After 4 h, $CaCl_2$ (100-fold excess) was added. The sample was then dialyzed overnight against deionized $H_2O$, centrifuged to remote precipitate, and lyophilized. The yield of N-7 was greater than 80% as determined by analysis of the released amino acids (see Results).

### *Instrumental Methods*

*Optical Stopped-Flow Spectroscopy.* The rate constants of Yb(III) release from the various Yb-bound parvalbumins were measured on a Durram-Gibson 13000 stopped-flow apparatus interfaced to a Nicolet Instruments Explorer IIIA digital oscilloscope. Data collection, using micromolar concentrations of the chelating dye xylenol orange and parvalbumin (pH 6.6; 150 mM KCl/15 mM Pipes; 23 °C), and data analysis, using double-exponential functions to fit the observed increase in absorbance at 570 nm, were performed as described by Corson et al. (1983a,b).

*$^1$H NMR Spectroscopy.* High-resolution 300-MHz $^1$H NMR spectra of native parvalbumin and its proteolytically shortened derivatives were acquired on a Nicolet Instruments NT-300WB spectrometer. Typical acquisition parameters were as follows: probe size = 5 mm; protein concentration = 0.5–2.5 mM; sample volume = 500 μL; spectral width = ±2000 Hz/16K data points; pulse length = 8 μs; preacquisition delay = 100 μs; free induction decay filter = Bessel (±3000 Hz) with quadrature phase detection; number of acquisitions = 1000–5000; resolution enhancement = Lorentzian to Gaussian. Desalted lyophilized protein samples were dissolved in 150 mM KCl/$D_2O$ at 23 °C, lyophilized once to reduce the residual HDO content, and then redissolved in the same volume of unsalted $D_2O$; lyophilized protein samples that had previously been dialyzed against KCl or NaCl were twice dissolved in an appropriate amount of $D_2O$ to ensure adequate ionic strength (100–200 mM KCl equivalent). Lu(III) titrations of the N-1, N-2, and N-7 derivatives were performed at 40, 55, and 40 °C, respectively, with the methods described by Corson et al. (1983b). All chemical shifts were referenced to the principal resonance of DSS.

Yb(III)-shifted 270-MHz $^1$H NMR spectra of native parvalbumin and its proteolytically shortened derivatives were acquired on a Bruker HXS-270 spectrometer. Typical acquisition parameters were as follows: probe size = 5 mm; sample volume = 400 μL; protein concentration = 1 mM; spectral width = ±10 000 Hz/32K data points; pulse length = 10 μs; preacquisition delay = 25 μs; FID filter = Bessel (±20 000 Hz) with quadrature phase detection; number of acquisitions = 50 000; signal-to-noise enhancement = 5 Hz; resolution enhancement = Lorentzian to Gaussian. Samples were prepared as described above; $YbCl_3$ (in $D_2O$) was then added to each sample to give a Yb:parvalbumin ratio of 0.7, and spectra were recorded at 30 °C (Lee & Sykes, 1981, 1983; Lee et al., 1985).

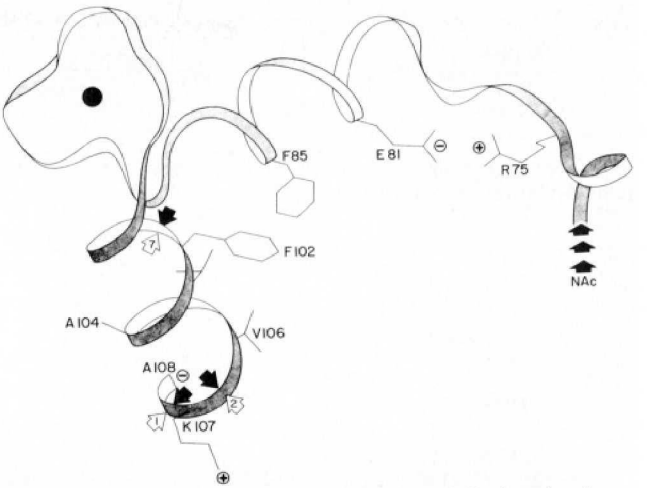


FIGURE 1: Ribbon drawing of the EF helix–loop–helix domain of carp parvalbumin [derived from the atomic coordinates of this protein as determined by Kretsinger & Nockolds (1973)]. Several of the side chains are shown as stick structures to emphasize their relative positions. The CPase A and CPase B cleavage points that yield the N-1, N-2, and N-7 derivatives are indicated by double arrows. The chelated Ca(II) ion is represented by the solid circle.

## RESULTS

*Proteolysis of Parvalbumin's F Helix.* The helix E–loop–helix F Ca(II)-binding site at parvalbumin's C-terminus is shown as a ribbon structure in Figure 1; the CPase A and CPase B cleavage points that resulted in the N-1, N-2, and N-7 derivatives are indicated by double-headed arrows. Since studies showed that Ca(II)-bound parvalbumin was not susceptible to proteolysis by the carboxypeptidases, apoparvalbumin was prepared. Unchecked digestion of the F-helix residues by relatively high levels of CPase A showed an initial fast release of Ala-108 followed by a considerably inhibited release of Lys-107, consistent with the known specificity of CPase A (Figure 2A). Removal of Lys-107, however, was quickly followed by loss of the remaining five neutral residues of parvalbumin's F helix. At lower enzyme concentrations, proteolysis was expectedly more controlled, digestion being limited to Ala-108. Due primarily to incomplete decalcification of parvalbumin, release of Ala-108 varied from 0 to 100%; high-yield products (i.e., 80–100% Ala-108 release) showed 0–10% release of lysine or subsequent residues as determined by the amino acid analysis of the digestion mixture. The characteristic heat stability of Ca(II)-loaded parvalbumins was not diminished in the N-1 form. Nor did dialysis against deionized $H_2O$ denature the Ca(II) form of N-1.

The time course of the CPase B digestion of des-Ala$^{108}$-parvalbumin is shown in Figure 2B. Under the conditions defined, 95% release of the C-terminal Lys-107, on the basis of the variable (80–100%) N-1 content of the starting material, could be achieved in 20 min without proteolysis of residues 106–102. Although the $Ca(II)_2$ form of N-2 was quite heat stable in the presence of 100–200 mM KCl, it precipitated at room temperature in low ionic strength solutions.

CPase A digestion of the N-2 derivative produced a mixture of intermediate-length parvalbumins. As shown in Figure 2C, Leu-105 and Ala-104 were released quickly, being nearly

Table I: Relative Amounts of the Amino Acids Released by the Renewed CPase A Digestion of N-3/N-4 and N-5/N-6 Mixtures

| N derivative | Lys-107 | Val-106 | Leu-105 | Ala-104 | Thr-103 | Phe-102 |
|---|---|---|---|---|---|---|
| N-3/N-4[a] | 0 | 0 | 0.76 | 1.01 | 1.03 | 1.00 |
| N-3/N-4[b] | 0.14 | 0.22 | 0.60 | 1.00 | 0.90 | 1.00 |
| N-5/N-6[c] | 0 | 0 | 0.25 | 0.25 | 0.90 | 1.00 |

[a] From DEAE-cellulose separation, peak III (Figure 3B). [b] From Yb(III)-precipitation method (see Experimental Procedures). [c] From DEAE-cellulose separation, peak II (Figure 3A).

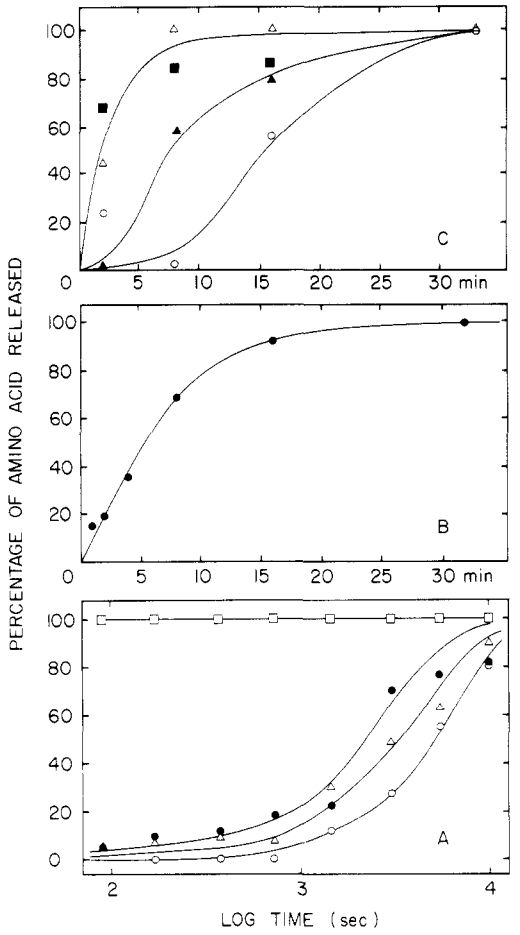


FIGURE 2: Carboxypeptidase-mediated digestions of parvalbumin. (A) Time course of the digestion of N by CPase A. Aliquots for amino acid analyses were taken before addition of enzyme, immediately after addition of enzyme and at the times indicated above. Apoparvalbumin (0.2 mM) and CPase A (200 units) in 10 mM $(NH_4)_2CO_3$/100 mM KCl, pH 6.5, 23 °C. Release of Ala-108 [(□) corrected by an amount equal to the molar average of Leu-105 and Thr-103 to account for the release of Ala from position 104], Lys-107 (●), the average of Val-106 + Leu-105 + Ala-104 + Thr-103 (△), and Phe-102 (○) is plotted as percentages of their maximum possible molar amounts vs. time. (B) Time course of the digestion of N-1 by CPase B. Des-Ala$^{108}$-parvalbumin (0.8 mM) and carboxypeptidase B (2 units) in 10 mM $(NH_4)_2CO_3$/100 mM KCl, pH 6.7, 20–23 °C. Amino acid aliquots were removed both before and after enzyme addition and at the times indicated above. Lys-107 (●) release is plotted as percent maximum molar amount vs. time. (C) Time course of the digestion of N-2 by CPase A. Carboxypeptidase A (20 units) was added to the 40-min CPase B/N-1 incubation mixture (see Figure 3). Aliquots for amino acid analyses were removed prior to the readdition of CPase A and at the times indicated above. Leu-105 (△), Ala-104 (■), Thr-103 (▲), and Phe-102 (○) releases are plotted as percent maximum molar amount vs. time.

complete within 10 min. Thr-103 release lagged moderately, being only 67% complete by 10 min. However, Phe-102 release lagged considerably, taking more than 30 min to reach its maximum. (The amino acid analyses of Val-106 release were unexpectedly variable.) Figure 3 illustrates DEAE column elution profiles of two 2–4-min CPase A incubation products of N-2. Peak I in both profiles eluted at a position coincident

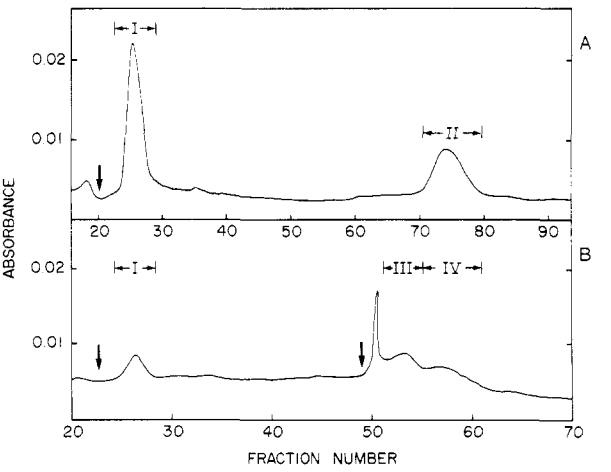


FIGURE 3: Elution profiles of the DEAE-cellulose separation of parvalbumin digestion products. (A) Trial 1 (single KCl gradient elution; 0–0.3 M) giving predominantly a mixture of N-5/N-6 in peak II (see Results and Table I). (B) Trial 2 (double KCl gradient elution; 0–0.2 and 0.1–1.0 M) giving predominantly a mixture of N-3/N-4 in peak III; the sharp peak that preceded peak III in (B) contained no protein. The start of the gradient elutions are indicated by arrows (see text).

with native Ca(II)-bound parvalbumin; its $^1H$ NMR spectrum (not shown) confirmed it to be a mixture of N and N-1. Peak II in Figure 3A was a mixture as shown by the amino acids released during renewed CPase A digestion of their already truncated F helices (Table I). Because CPase-mediated digestion of parvalbumin beyond Phe-102 is effectively inhibited by the acid side chains of Glu-101 and Asp-100, the renewed proteolysis of isolated N-3 through N-6 intermediates should release into solution only those residues of helix F that remain after the initial CPase A/CPase B/CPase A treatment. As shown in Table I, no valine was released from peak II, indicating the absence of undigested N-2; in addition, very little leucine or alanine was detected, indicating that the initial proteolysis sequence had progressed nearly completely to the level of N-5. The relative abundance of threonine and phenylalanine liberated by the renewed CPase A digestion confirmed that peak II was predominantly N-5, the N-6 content being an estimated 20%. Similarly, because peak III in Figure 3B yielded nearly equivalent amounts of Ala, Thr, and Phe but only 0.75 as much Leu, the relative excess of Ala, Thr, and Phe was attributed to N-4 present as the minor component in a 1:3 mixture with N-3. Taking into account an estimated 20% N/N-1 contamination (as determined from its $^1H$ NMR spectrum; not shown), the composition of peak III was calculated to be a 20:60:20 mixture of (N + N-1)/N-3/N-4 (see Table I). The product isolated by the Yb(III)-precipitation method was determined to be a 14:10:36:40 mixture of N-1/N-2/N-3/N-4 (see Table I).

The two acidic residues at positions 101 and 102 effectively retarded carboxypeptidase A digestion of apoparvalbumin; less than 3% of these residues were released under conditions where N-7 was produced. This is analogous to the controlled digestion of tropomyosin used in the preparation of its nonpolymerizable form (Mak & Smillie, 1981).

Table II: Kinetic and Thermodynamic Data of Lanthanide(III) Binding to Parvalbumin and Its Derivatives

| derivative | $k_{CD}$[a] | $k_{EF}$[a] | $\Delta I_{EF}/\Delta I_{CD}$[b] | $\beta_{CD}$[c] | $\beta_{EF}$[c] |
|---|---|---|---|---|---|
| N | 0.15 ± 0.03 | 0.00133 ± 0.0001 | 3.2 | 11 | 83 |
| N-1 | 0.13 ± 0.04 | 0.00152 ± 0.0004 | 3.7 | 33 | 1000 |
| N-2 | 0.094 ± 0.004 | 0.00116 ± 0.00006 | 1.8 | 25 | 500 |
| N-3/N-4[d] | 0.35 ± 0.08 | 2.9 ± 0.7 | ND | ND | ND |
| N-5/N-6 | | 3.8 ± 0.4 | ND | ND | ND |
| N-7 | | 1.6 ± 0.2 | ND | ND | ND |

[a] Yb(III) off-rate constants determined from optical stopped-flow studies of solutions of Yb parvalbumin at approximately 1:1, in $s^{-1}$. [b] Relative intensities of the slow [release of Yb(III) from the EF site] and fast [release of Yb(III) from the CD site] phases; ND, not determined. [c] Lu(III) binding constants relative to $\beta_{Ca}$ (i.e., $\beta_{Lu}/\beta_{Ca}$), determined from $^1$H NMR-monitored Ca(II)/Lu(III) exchange studies. [d] Tentative assignment of $k_{off}$ (see text).

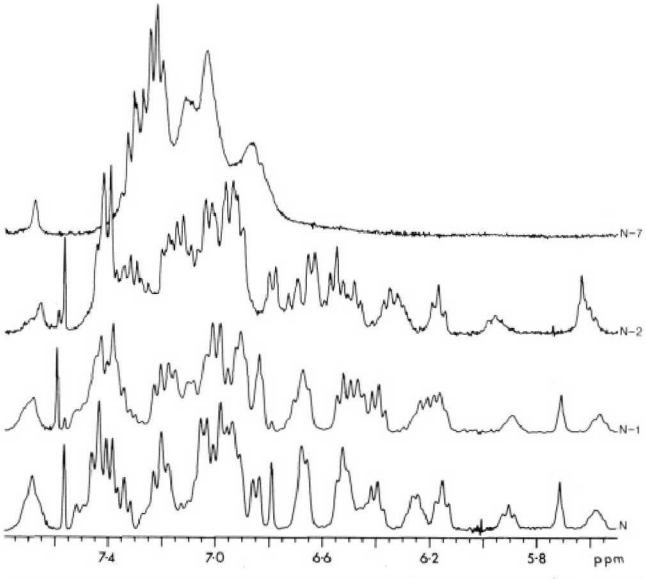


FIGURE 4: Aromatic region (7.8–5.5 ppm) of the 300-MHz $^1$H NMR diamagnetic spectra of carp parvalbumin (N) and its proteolytic derivatives (N-1, N-2, and N-7). All samples were recorded in 100–200 mM $KCl/D_2O$, pH 6.8; the spectra of N, N-1, and N-7 were recorded at 40 °C whereas the spectrum of N-2 was recorded at 55 °C.

*Lanthanide(III) Binding.* Lanthanide(III) ions compete extremely effectively for the Ca(II)-binding sites in many classes of proteins (Williams, 1970; Smolka et al., 1971; Matthews & Weaver, 1974; Brittain et al., 1976; Kretsinger & Nelson, 1976; Martin, 1983; Levine, 1983), a phenomenon attributed primarily to a combination of the higher charge density of Ln(III)'s and their preference for oxygen–ligand chelation. In the case of the parvalbumins, the two bound Ca(II) ions are readily displaced by any member of the lanthanide(III) series of ions (Corson et al., 1983b). However, the helix C–loop–helix D domain markedly prefers the larger lanthanides whereas the helix E–loop–helix F domain is nonselective, this difference in selectivities resulting in preferential loading of the EF site by the smaller Ln(III)'s [e.g., Yb(III) or Lu(III)] at Ln(III):parvalbumin ratios less than 1 (Lee & Sykes, 1981; Corson et al., 1983a; Williams et al., 1984).

*$k_{off}$ Determinations.* Solutions of native parvalbumin to which approximately 1 molar equivalent of Yb(III) has been added show two distinct phases of Yb(III) release by optical stopped-flow methods: a fast phase assigned to release of Yb(III) from the CD site, $k_{CD} = 0.15\ s^{-1}$, and a slow phase, approximately 3 times as intense as the fast phase, assigned to release of Yb(III) from the EF site, $k_{EF} = 0.00133\ s^{-1}$ (Corson et al., 1983a). At a lanthanide:parvalbumin ratio of ~1, the kinetics of Yb(III) release from N-1 and N-2 were remarkably similar to the biphasic release observed for N (Table II). Not only have the absolute values for these

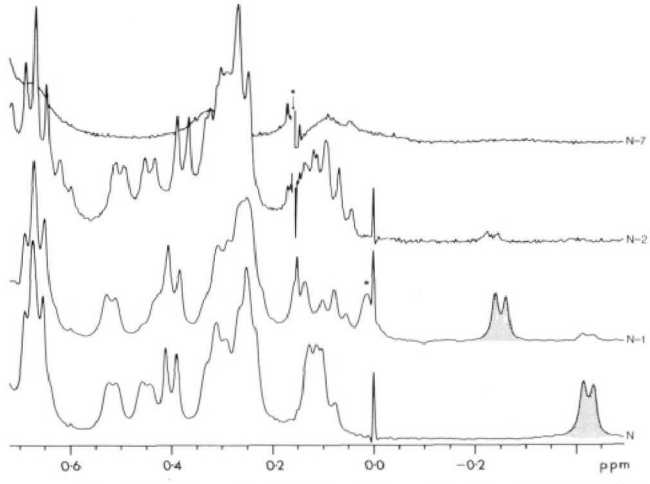


FIGURE 5: Aliphatic region (0.7 to −0.5 ppm) of the 300-MHz $^1$H NMR diamagnetic spectra of carp parvalbumin (N) and its proteolytic derivatives (N-1, N-2, and N-7). All samples were dissolved in 100–200 mM $KCl/D_2O$, pH 6.8; the spectra of N, N-1, and N-7 were recorded at 40 °C whereas the spectrum of N-2 was recorded at 55 °C. The shaded resonance in the spectra of N and N-1 has been tentatively assigned to the γ-2 methyl group of Val-106 (see Results).

off-rate constants changed by less than 36% [$k_{CD} = 0.15\ s^{-1}$ (N), $0.13\ s^{-1}$ (N-1), and $0.094\ s^{-1}$ (N-2); $k_{EF} = 0.00133\ s^{-1}$ (N), $0.00152\ s^{-1}$ (N-1), and $0.00116\ s^{-1}$ (N-2)], but the relative intensity of the two phases has also changed very little ($2 < \Delta I_{EF}/\Delta I_{CD} < 4$), indicating continued preference of Yb(III) for the EF site. The mixture of N-3/N-4 derivatives showed drastically altered Yb(III) dissociation rates. The large increase in rates for both slow and fast stages of Yb(III) release makes the assignment of particular phases to specific sites ambiguous. For the assignment indicated in Table II, $k_{CD}$ has increased by a factor of 2, whereas $k_{EF}$ has increased by a factor of 2200. For the reverse assignment, the increases are by factors of 20 and 260, respectively. The mixture of N-5/N-6 derivatives showed an even greater deviation from normal kinetics. Only one rather fast $k_{off}$ was observed for this mixture, the $3.8\ s^{-1}$ rate of release being approximately 25 times faster than the fastest $k_{off}$ from uncleaved parvalbumin. The N-7 derivative was similar to the N-5/N-6 mixture in that it, too, showed only one fast-release phase, approximately 11–1200 times the values of $k_{off}$ normally observed.

*β Determinations.*[2] The high-resolution 300-MHz $^1$H NMR spectra of the Ca(II)-saturated forms of both N-1 and

[2] In accordance with the standard convention of expressing metal ion complex equilibria as formation reactions (IUPAC Comission on Equilibrium Data, 1979), the metal complexes of parvalbumin are described here in terms of their overall stability constants, β, rather than as dissociation constants, $K_d$, as has been done frequently in the past. Stability constants referred to in this work are identified by a double index: the first subscript indicates the type of metal ion bound; the second specifies which site in parvalbumin is involved in chelation.

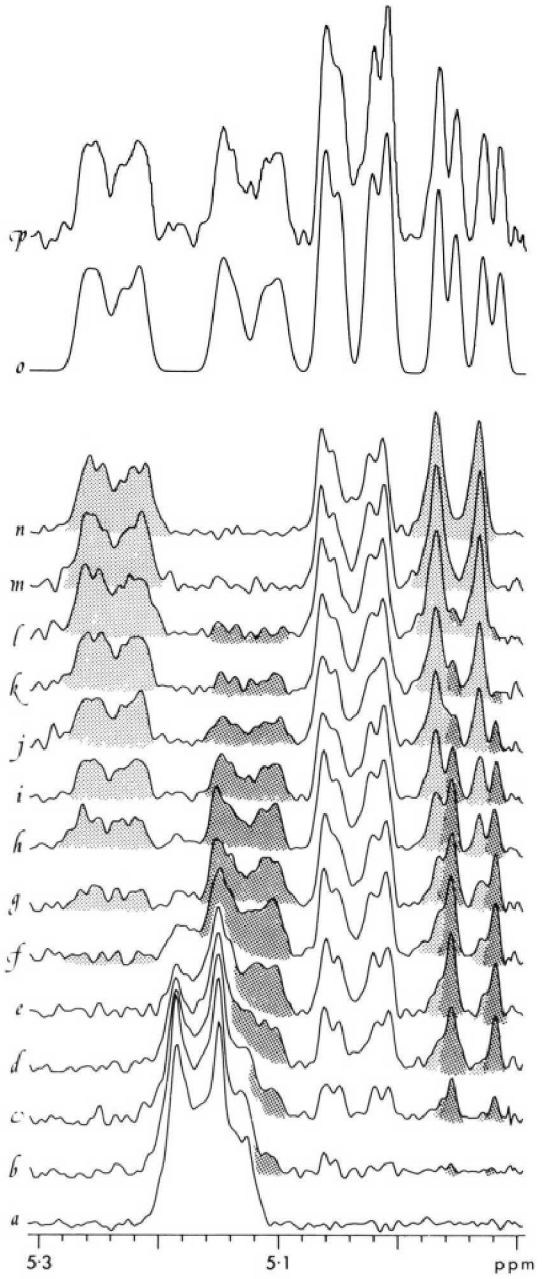


FIGURE 6: Stacked plot of the change in the downfield-shifted $\alpha$-CH region (5.3–5.0 ppm) of the 300-MHz $^1$H NMR spectrum of N-2 caused by Lu(III) titration of the Ca(II) form of the protein. Those resonances shaded lighter gray arise from the sum of the $Lu_2$ and Lu(CD):Ca(EF) species whereas those resonances shaded darker gray arise from the intermediate Ca(CD):Lu(EF) species. The Lu(III):parvalbumin ratios are as follows: a, 0.00; b, 0.104; c, 0.313; d, 0.521; e, 0.729; f, 0.937; g, 1.146; h, 1.354; i, 1.563; j, 1.771; k, 1.979; l, 2.188; m, 2.396; n, 2.604. Trace h is replotted on an expanded scale as trace p above its calculated version determined by Gaussian line-shape curve analysis (trace o).

N-2 (Figures 4 and 5) indicate that, like N, their tertiary structures in solution are well-defined. The presence of upfield-shifted methyl group resonances (from 0.8 to −0.4 ppm) and the spread of resonances in the aromatic region (from 7.6 to 5.0 ppm) are quite characteristic of the folded conformation native parvalbumins assume. Note that the farthest upfield-shifted methyl resonances in N (the doublet at −0.430 ppm) appears most sensitive to removal of Ala-108, moving downfield by about 0.2 ppm. In the spectrum of N-2, this resonance has again shifted at least another 0.3 ppm downfield relative to its position in N-1, becoming lost in the overlap of multiplets between 0.8 and 0.0 ppm. No other resonance suffered an

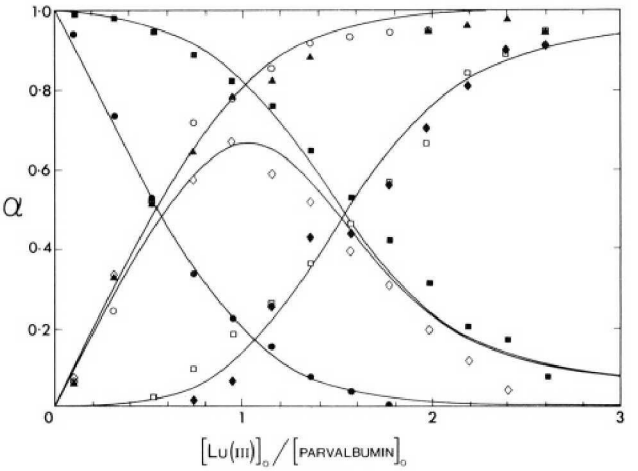


FIGURE 7: Lu(III) titration data of N-2 carp parvalbumin. Relative peak areas ($\alpha$) of four upfield-shifted methyl doublet resonances and three downfield-shifted $\alpha$-CH resonances (Figure 9) are plotted vs. the Lu(III):parvalbumin ratios listed in Figure 6. Overlying the data points are the theoretical distribution curves calculated from the binding constants obtained by a least-squares fit of the data: (■), 0.504 ppm methyl; (□), 0.485 ppm methyl; (●), 0.446 ppm methyl; (○), 0.433 ppm methyl; (♦), 5.237 ppm $\alpha$-CH; (◊), 5.122 ppm $\alpha$-CH; (▲), 5.039 ppm $\alpha$-CH.

apparent shift of this magnitude. As judged from the relative integrated areas of this particular doublet resonance, the N-1 preparation was an 86:14 mixture of N-1/N whereas the N-2 preparation was an 85:12:3 mixture of N-2/N-1/N (see Figure 5). Because the calculation of binding constants from $^1$H NMR derived Ca(II)/Lu(III) exchange data depends entirely on such spectral features, the lack of shifted, well-resolved resonances in the spectra of the N-7 derivative (Figures 4 and 5) and N-3/N-4 and N-5/N-6 derivative mixtures (not shown) precluded the determination of their Lu(III) binding constants.

The methyl doublets at 0.525 and −0.239 ppm, and the $C_2$-H singlet resonance of His-26 at 7.593 ppm in the spectrum of N-1 (Figures 4 and 5) showed easily analyzed intensity decreases throughout the Lu(III) titration of this derivative. Associated with each of these decreasing resonances was an increasing resonance of similar line width and multiplet pattern. Both the doublet at −0.239 ppm and the singlet at 7.593 ppm decreased rapidly from the onset of titration; a doublet at −0.201 ppm and a singlet at 7.604 ppm rose in their place. The decrease of the doublet at 0.525 ppm lagged considerably during the first phase of the Lu(III) titration (i.e., from 0 → 1 Lu(III):parvalbumin) but became much more rapid during the latter phase (i.e., from 1 → 2 Lu(III):parvalbumin). The relative values of the Lu(III) binding constants, calculated from these observed intensity changes as described by Corson et al. (1983b), are listed in Table II; they show little change from the published values, $\beta_{EF}$ being slightly more sensitive to loss of Ala-108 than was $\beta_{CD}$.

In addition to the decreases in the two well-resolved doublet resonances at 0.504 and 0.446 ppm and the concomitant increases in their replacement resonances at 0.485 and 0.433 ppm, respectively, the intensity changes undergone by three $\alpha$-CH resonances were used to calculate the Lu(III) $\beta$'s for N-2 parvalbumin (Figures 6 and 7). $\alpha$-CH resonances in this downfield-shifted region of the spectrum have been attributed to those residues that participate in $\beta$-sheet formation and have been used to give some indication of the folded state of a protein (Dalgarno et al., 1983a,b); the antiparallel chains of the CD and EF loops presumably form a short (3–4 H-bonded) segment of $\beta$-structure (Sowadski et al., 1978). In particular, note the lag in the development of the $\alpha$-CH resonance at

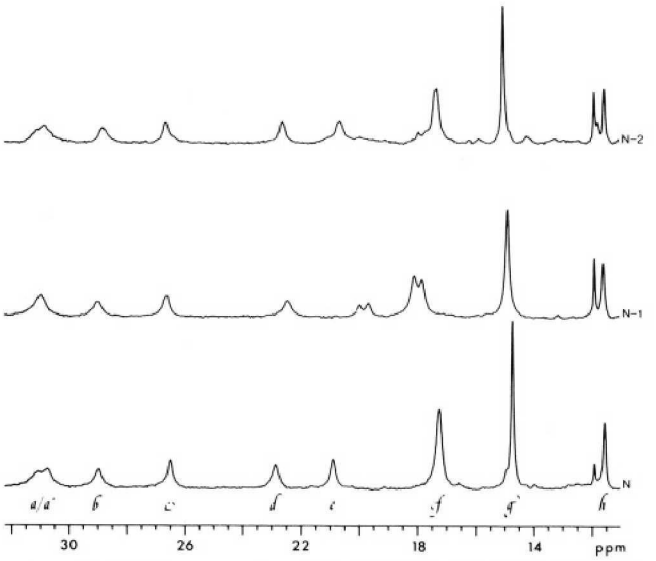


FIGURE 8: 32–11 ppm region of the Yb(III)-shifted 270-MHz $^1$H NMR spectra of carp parvalbumin (N), N-1, and N-2 (150 mM KCl, pH 6.8, 30 °C). The Yb(III):parvalbumin ratio was approximately 0.7 for all samples.

5.237 ppm, the rise and fall of the resonance at 5.122 ppm, and the immediate development and leveling off of the doublet of doublets $\alpha$-CH resonance at 5.039 ppm.

In exact analogy to the curve-fitting methods described previously (Williams et al., 1984), each spectrum in the set of the Lu(III) N-2 titration series was analyzed as discrete multiplet sets of Gaussian line shapes (Figure 6, curves o and p). The areas of each multiplet set (normalized to the maximum calculated area of the resonance at 5.039 ppm) represent the fractions of the various Ca(II)- and Lu(III)-bound forms of N-2 present at a given Lu(III):parvalbumin ratio (Figure 7). The resonance at 5.237 ppm arose from the N-2 species in which Lu(III) was bound to both the CD and EF sites, the resonance at 5.122 ppm arose from the N-2 species in which Lu(III) was bound only to the EF site, and the resonance at 5.039 ppm arose from the N-2 species that bind Lu(III) at the EF site regardless of whether Ca(II) or Lu(III) is bound to the CD site. The sharper doublet resonance at 4.935 ppm also followed the fate of an intermediate Ca(II):Lu(III) N-2 species; the doublet resonance at 4.945 ppm presumably comes from this same $\alpha$-CH proton of N-2 in the $Lu_2$ form. The calculated Lu(III) $\beta$'s for N-2 are listed in Table II; they indicate not only that this clipped form of parvalbumin is still quite capable of strongly binding two Ca(II) or Lu(III) ions but also that the EF site is still preferentially loaded with Lu(III).

*EF Domain Structures.* The Yb(III)-shifted $^1$H NMR resonances of $Ca_1Yb_1$ parvalbumin provide extremely sensitive indications of structural change in the EF domain (Lee & Sykes, 1980–1983; Lee et al., 1985). Figures 8–10 show comparisons of three well-resolved regions of the Yb(III)-shifted spectra of N, N-1, and N-2. The great similarity in all regions of their spectra imply that the structures of the EF domain in these derivatives are extremely similar. One for one comparisons of most of the labeled resonances (a–d, g, h, j, l–q, and s–z) indicate that, within at least 10 Å of the Yb(III) ion, the protein has suffered no significant change in structure (<0.2 Å).

However, several spectral differences are evident. Although resonances e and f at 20.88 and 17.22 ppm in the spectrum of N (Figure 8) are nearly unaffected in the spectrum of N-2 (20.55 and 17.37 ppm), they are different in the spectrum of

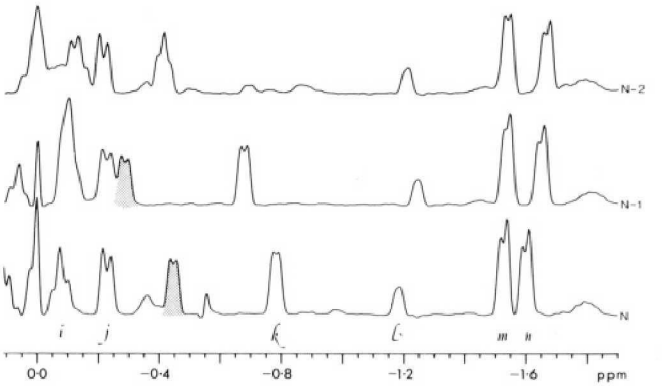


FIGURE 9: 0–2 ppm region of the Yb(III)-shifted 270-MHz $^1$H NMR spectra of carp parvalbumin (N), N-1, and N-2. The experimental conditions were the same as in Figure 8. The shaded resonance in N and N-1 corresponds to the shaded resonance in the respective spectrum of each in Figure 5.

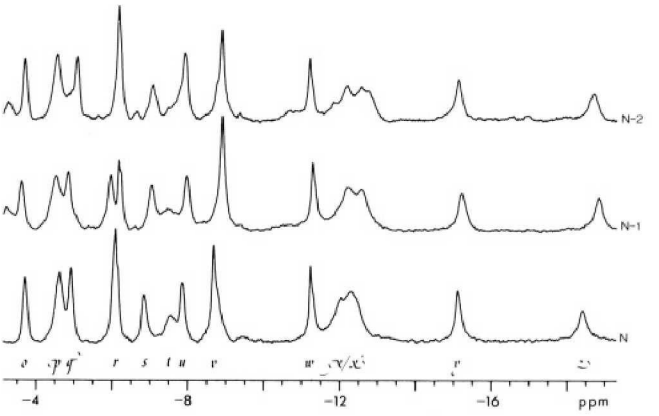


FIGURE 10: −3 to −20 ppm region of the Yb(III)-shifted 270-MHz $^1$H NMR spectra of carp parvalbumin (N), N-1, and N-2. The experimental conditions were the same as in Figure 8.

N-1. The singlet e resonance (relative area = 1) and singlet f resonance (relative area = 3) both split into apparent doublet resonances centered at 19.80 and 17.95 ppm, respectively. Determination of the principal axis system of the magnetic susceptibility tensor of the EF-bound Yb(III) has allowed Lee and Sykes (1983) to assign resonance f to the $\delta$-1 methyl group of Leu-86; calculations of the paramagnetic shifts for other EF-domain protons indicate that resonance e may arise from one of the $\gamma$-$CH_2$ protons of Ile-97 or one of the $\beta$-$CH_2$ protons of Asp-90 (Lee & Sykes, 1983). The separation of the peaks in these doublets (83 Hz for e; 77 Hz for f) is neither equal nor within the normal range of H–H scalar couplings and may arise from slow exchange of the Leu-86 and other side chains between two different orientations relative to the bound-Yb(III).

Of all the resonances illustrated in Figures 8–10, only the doublets at −0.45 and −0.25 ppm in the spectra of N and N-1, respectively (Figure 9), arise from the $Ca_2$ forms of these proteins. These methyl doublet resonances appear in the normal spectra of N and N-1 as their most upfield-shifted peaks (Figure 5; the shaded resonances). Their relative intensities in Figure 9 are quite consistent with the calculated proportion of the $Ca_2$ form present in a solution of Yb(III) parvalbumin with ratio ~0.7. Note that the slight downfield diamagnetic shift of this resonance in the N-1 form is apparently accompanied by a nearly equivalent shift in position of the Yb(III)-shifted resonance at approximately −0.77 ppm in N. Furthermore, the movement of the diamagnetic resonance out of this spectral region in the spectrum of N-2 (see Figure 5) also results in the apparent loss of this accompanying

paramagnetically shifted resonance. For these reasons, the resonances at −0.77 and −0.65 ppm in the spectra of N and N-1, respectively, are tentatively attributed to the methyl group of that residue which gives rise to the shaded resonances in the diamagnetic spectra. Because the methyl doublet resonance at −0.45 ppm in the spectrum of carp parvalbumin is very sensitive to digestion of the F helix and because the analogous resonance at −0.30 ppm in the spectrum of pike III parvalbumin is very sensitive to protonation of His-106 (Williams et al., 1986), we have tentatively assigned these resonances to the γ-2 methyl group of Val-106 as was initially suggested by Parello et al. (1974) on the basis of ring-current secondary shift calculations, rather than to Leu-67 as was later speculated by Birdsall et al. (1979). Assignment to Val-106 is consistent both with this resonance's greater sensitivity to metal ion exchange at the EF site as determined by Corson et al. (1983a) and with the relatively small paramagnetic shift calculated for the γ-2 methyl group in the $Yb_1Ca_1$ form of the protein (0.17 ppm; Lee & Sykes, 1983).

Because the relative intensity of peak r in the spectra of N and N-2 (Figure 10) is nearly twice that of most other resonances in the −3 to −20 ppm region, we assume it arises from the coincidental overlap of two single-proton Yb(III)-shifted resonances. The apparent splitting of r in the N-1 spectrum is, therefore, attributed to the resolution of these overlapping resonances due to slight changes in the paramagnetic contributions to their chemical shifts.

## Discussion

Carboxypeptidase-mediated digestions of the C-terminal region of proteins have in the past provided useful insights into structure–function relationships. Morgan and Riehm (1968) and Gerken et al. (1982) have shown that removal of hen egg white lysozyme's two C-terminal nonhelical residues, Leu-129 and Arg-128, by successive CPase A and CPase B digestions can significantly alter this enzyme's catalytic activity under varying conditions of ionic strength and pH. Sardana and Breslow (1984) have also used $^1$H NMR spectroscopy to determine the effect of the CPase-mediated loss of neurophysin I's three C-terminal residues. Using similar strategy, we have successfully generated several derivatives of carp parvalbumin that differ only in the length of their C-terminal F helix.

As readily discerned from its crystal structure, carp parvalbumin's F helix appears bound to the protein fold through a periodic series of hydrophobic contacts between its side chains (Val-99, Phe-102, Leu-105, and Val-106) and those of numerous residues from helix B, the BC-linker region and helix C (Moews & Kretsinger, 1975). In addition, model-building studies indicate that the free carboxyl group at the C-terminus (Ala-108) may form a salt-bridge with the $\epsilon$-$NH_3^+$ group of Lys-27. Lys-27 of carp parvalbumin is, in fact, highly conserved throughout both the α- and β-lineages. Although α-parvalbumins are in most cases one residue longer than β-parvalbumins, extending the C-terminal turn of helix F, the ion pair carboxyl complement may be provided not by the C-terminus itself but rather by the side chain of the nearly invariant Glu-108 found in α-parvalbumins. Such protein-stabilizing structural features are, of course, not without precedence. The compactness of myoglobins and hemoglobin subunits forces their eight α-helical structures close together. X-ray studies of sperm whale metmyoglobin suggest that 9 out of 11 invariant lysine residues found in each of 24 sequenced myoglobins are involved in salt-bridge interactions, 7 serving to directly stabilize helix–helix or helix–linker contacts (Takano, 1977). In addition to similar intramolecular interactions, deoxyhemoglobin's subunits are stabilized by sets of intermolecular salt bridges (Baldwin & Chothia, 1979). The close pack of the $\beta_1$ (or $\beta_2$) subunit's C-terminus with the side chain of Lys-40 on the $\alpha_2$ (or $\alpha_1$) subunit creates a salt bridge that contributes to the deoxy form's rigidity. That such X-ray detected salt bridges persist in the solution structure of a protein is also supported by Gerken's et al. (1982) study of des-Leu$^{129}$,Arg$^{128}$-lysozyme. In its unproteolyzed form, the NMR resonances of the $^{13}$C-enriched dimethylated Lys-13 of lysozyme titrate with a $pK_a$ of 9.8; in its proteolyzed form, Lys-13's $pK_a$ drops to 9.3, suggesting loss of the X-ray-detected (Browne et al., 1969) ion pair interaction with the C-terminus. Hydrophobic contacts that stabilize helix–helix interactions are no less important. Of the 35 or so Phe, Leu, Ile, and Val residues in myoglobin that contribute to its three interhelical hydrophobic clusters, 22 are invariant.

Stepwise removal of residues from the F helix of parvalbumin was undertaken as a means of assessing the particular significance of these various helix–helix interactions. Both kinetic and thermodynamic data [i.e., Ln(III) off-rates and binding constants] as well as the information gleaned from the diamagnetically and paramagnetically shifted $^1$H NMR spectra indicate that N,N-1, and N-2 are exceedingly similar in both functional and structural aspects. Deletion of any or all of the remaining F-helix residues, however, seriously impairs the metal ion binding capability of parvalbumin with concomitant gross alterations in its solution structure. A plausible interpretation of what transpires is as follows. In N, there exists an ion pair bond between the protonated $\epsilon$-$NH_3^+$ of Lys-27 (a solvent-oriented residue on helix B; Kretsinger & Nockolds, 1973) and negatively charged C-terminal $COO^-$ group of Ala-108. Hydrolysis of the Lys-107–Ala-108 peptide bond produces a surrogate C-terminus, which, because of its location on the solvent side of helix F, is still well positioned to reestablish the ion pair bond with Lys-27. In so doing, the shortened F helix is rotated slightly toward Lys-27. This rotation is apparently transmitted to the loop region, the side chains of Leu-86, and another residue (possibly Ile-97) exhibiting slow exchange between two marginally different environments. Hydrolysis of the Val-106–Lys-107 peptide bond also produces an available, charged C-terminus. However, because the new C-terminus arises more from the underside of helix F, ion pair bond formation with Lys-27 rotates the helix in the opposite sense as was done by N-1, resulting in a structure that in some ways is more similar to N than was N-1. Persistence of this salt bridge through the N-2 form is consistent with the relative resistance of the metal-bound forms of these derivatives to digestion by carboxypeptidases. The facile CPase-mediated digestion of the apo forms of N, N-1, and N-2 as well as the metal-bound forms of N-3 through N-6 suggests that this particular ion pair bond is weak or nonexistent in these forms. In addition, the C-terminal end of helix F appears to be stabilized not only by its interaction with Lys-27 of helix B but also by a H bond between the $\epsilon$-$NH_3^+$ group of Lys-107 and a backbone C=O or seryl −OH in the BC-linker region (residues 32–36; Figure 11). This we conclude from the work of Williams et al. (1986), who have shown significant conformational sensitivity of several B-helix residues to deprotonation of His-106, Lys-107's analogue in pike III parvalbumin.

Further dimunition of helix F not only deprives this secondary structural unit the stability endowed it by the ion pair interaction and the axially oriented H bonds but also reduces the potential number of hydrophobic interactions that exist on its core-side surface. The most striking observation of these proteolytic experiments is the marked sensitivity of the CD

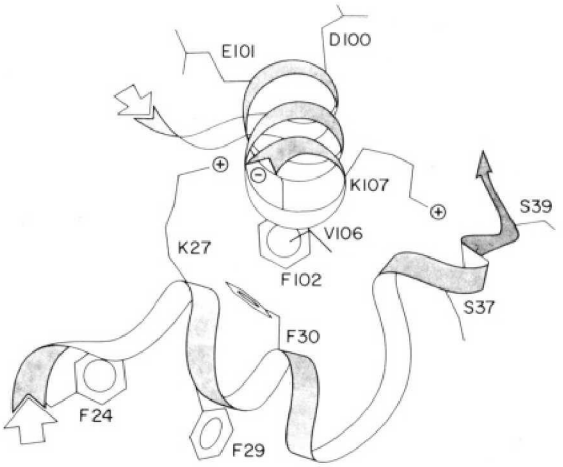


FIGURE 11: Ribbon drawing of the interaction of the F and B helices of carp parvalbumin. The ion pair bond between the C-terminus and Lys-27 and the proposed H bond between Lys-107 and an undetermined BC-linker region residue are emphasized.

site's metal ion binding capability to modifications of one of the EF site's helices. Because the F helix was modified by degradation rather than by amino acid substitution, it is impossible to assess to what extent loss of specific helix–helix hydrophobic contacts (vs. disruption of the EF substructure as a whole) destabilized the protein fold. However, the drastically increased rates of Yb(III) release for the N-3 through N-7 derivatives and the near invariance of residues Phe-102, Leu-105, and Val-106 attest to their significant role in helix–helix stabilization. In any case, it seems clear that efficient chelation of divalent or trivalent metals by such helix–loop–helix structures depends strongly on the mutual stabilization of helices afforded by paired domains.

## ACKNOWLEDGMENTS

We thank M. Natriss for analyses of the amino acid samples, Dr. Clive Sanders for advice concerning CPase A digestion, D. Bacon, M. Fujinaga, and C. McPhalen for generation of the ball-and-stick figures of carp parvalbumin's structure (MMS molecular graphics system) from which Figures 1 and 11 were drawn, and G. Sim and E. Metke for construction of the molecular model of carp parvalbumin.

**Registry No.** Yb, 7440-64-4; Lu, 7439-94-3; Ca, 7440-70-2.

## REFERENCES

Ambler, R. P. (1972) *Methods Enzymol. 25* (Part B), 143–154.

Baldwin, J., & Chothia, C. (1979) *J. Mol. Biol. 129*, 175–220.

Barker, W. C., Ketcham, L. K., & Dayhoff, M. D. (1978) in *Atlas of Protein Sequence and Structure* (Dayhoff, M. D., Ed.) pp 273–283, National Biomedical Research Foundation, Washington, DC.

Birdsall, W. J., Levine, B. A., Williams, R. J. P., Demaille, J. G., Haiech, J., & Pechère, J.-F. (1979) *Biochimie 61*, 741–750.

Bose, K., & Bothner-By, A. A. (1983) *Biochemistry 22*, 1342–1347.

Brittain, H. G., Richardson, F. S., & Martin, R. B. (1976) *J. Am. Chem. Soc. 98*, 8255–8260.

Browne, W. J., North, A. C. T., Philips, D. C., Brew, K., Vanaman, T. C., & Hill, R. L. (1969) *J. Mol. Biol. 42*, 65–86.

Cachia, P. J., Gariépy, J., & Hodges, R. S. (1985) in *Calmodulin Antagonists and Cellular Physiology* (Hidaka, H., & Hartshorne, P. J., Eds.) Chapter 5, pp 63–88, Academic Press, New York.

Corson, D. C., Lee, L., McQuaid, G. A., & Sykes, B. D. (1983a) *Can. J. Biochem. Cell Biol. 61*, 860–867.

Corson, D. C., Williams, T. C., & Sykes, B. D. (1983b) *Biochemistry 22*, 5882–5889.

Dalgarno, D., Drabikowski, W., Klevit, R., Levine, B., Scott, M., & Williams, R. (1983a) in *Calcium Binding Proteins* (deBernard, B., et al., Eds.) pp 83–91, Elsevier, New York.

Dalgarno, D., Levine, B. A., & Williams, R. J. P. (1983b) *Biosci. Rep. 3*, 443–452.

Folk, J. E., & Schirmer, E. W. (1963) *J. Biol. Chem. 238*, 3884.

Folk, J. E., Piez, K. A., Carroll, W. R., & Gladner, J. A. (1960) *J. Biol. Chem. 235*, 2272.

Fraenkel-Conrat, H., Harris, J. L., & Levy, A. L. (1955) *Methods Biochem. Anal. 2*, 339.

Gariépy, J., & Hodges, R. S. (1983) *FEBS Lett. 160*, 1–6.

Gerken, T. A., Jentoft, J. E., Jentoft, N., & Dearborn, D. G. (1982) *J. Biol. Chem. 257*, 2894–2900.

Haiech, J., Derancourt, J., Pechère, J.-F., & Demaille, J. G. (1979) *Biochimie 61*, 583–587.

Haner, M., Henzl, M. T., Raissouni, B., & Birnbaum, E. R. (1985) *Anal. Biochem. 138*, 229–234.

Herzberg, O., & James, M. N. G. (1985) *Nature (London) 313*, 653–659.

IUPAC Commission on Equilibrium Data (1979) *IUPAC Chem. Data Ser. No. 22* (Part B).

Kretsinger, R. H., & Nockolds, C. E. (1973) *J. Biol. Chem. 248*, 3313–3326.

Kretsinger, R. H., & Nelson, D. J. (1976) *Coord. Chem. Rev. 18*, 29–124.

Lee, L., & Sykes, B. D. (1980) *Adv. Inorg. Biochem. 2*, 183–210.

Lee, L., & Sykes, B. D. (1981) *Biochemistry 20*, 1156–1162.

Lee, L., & Sykes, B. D. (1982) in *Biochemical Structure Determination by NMR* (Bothner-By, A. A., Glickson, J. D., & Sykes, B. D., Eds.) pp 169–188, Marcel Dekker, New York.

Lee, L., & Sykes, B. D. (1983) *Biochemistry 22*, 4366–4373.

Lee, L., Corson, D. C., & Sykes, B. D. (1985) *Biophys. J. 47*, 139–142.

Levine, B. A., & Dalgarno, D. C. (1983) *Biochim. Biophys. Acta 726*, 187–204.

Mak, A. S., & Smillie, L. B. (1981) *Biochem. Biophys. Res. Commun. 101*, 208–214.

Martin, R. B. (1983) *Met. Ions Biol. 6*, 235–269.

Matthews, B. W., & Weaver, L. H. (1974) *Biochemistry 13*, 1719–1725.

Moews, P. C., & Kretsinger, R. H. (1975) *J. Mol. Biol. 91*, 201–228.

Morgan, W. T., & Riehm, J. P. (1968) *Biochem. Biophys. Res. Commun. 30*, 50–56.

Parello, J., Cavé, A., Puigdomenech, P., Maury, C., Capony, J. P., & Pechère, J.-F. (1974) *Biochimie 56*, 61–76.

Sardana, V., & Breslow, E. (1984) *J. Biol. Chem. 259*, 3669–3679.

Seamon, K. B., & Kretsinger, R. H. (1983) *Met. Ions Biol. 6*, 1–51.

Smolka, G. E., Birnbaum, E. R., & Darnall, D. W. (1971) *Biochemistry 10*, 4556–4561.

Sowadski, J., Cornick, G., & Kretsinger, R. H. (1978) *J. Mol. Biol. 124*, 123–132.

Sundaralingam, M., Bergstrom, R., Strasburg, G., Rao, S. T., Roychowdhury, P., Greaser, M., & Wang, B. C. (1985) *Science (Washington, D.C.) 227*, 945–948.

Szebenyi, D. M. E., Obendorf, S. K., & Moffat, K. (1981) *Nature (London) 294*, 327–332.
Takano, T. (1977) *J. Mol. Biol. 110*, 537–568.
Tschesche, H. (1977) *Methods Enzymol. 47* (Part E), 73–84.
Williams, R. J. P. (1970) *Q. Rev., Chem. Soc. 24*, 331.
Williams, T. C., Corson, D. C., & Sykes, B. D. (1984) *J. Am. Chem. Soc. 106*, 5698–5702.
Williams, T. C., Corson, D. C., McCubbin, W. D., Oikawa, K., Kay, C. M., & Sykes, B. D. (1986) *Biochemistry* (second paper of three in this issue).

# $^1$H NMR Spectroscopic Studies of Calcium-Binding Proteins. 2. Histidine Microenvironments in $\alpha$- and $\beta$-Parvalbumins As Determined by Protonation and Laser Photochemically Induced Dynamic Nuclear Polarization Effects†

Thomas C. Williams,* David C. Corson, William D. McCubbin, Kimio Oikawa, Cyril M. Kay, and Brian D. Sykes
*Medical Research Council of Canada Group in Protein Structure and Function and Department of Biochemistry, University of Alberta, Edmonton, Alberta, Canada T6G 2H7*

*Received July 18, 1985*

ABSTRACT: The microenvironments of the histidines in three isoforms of Ca(II)-bound parvalbumin (carp, p$I$ = 4.25; pike, p$I$ = 5.00; rat, p$I$ = 5.50) have been examined with $^1$H NMR techniques to probe their protonation characteristics and photochemically induced dynamic nuclear polarizability (photo-CIDNP). The histidine at position 26 (or 25), present in all three of these proteins, shows absolutely *no* photo-CIDNP enhancement of its $C_2H$ or $C_5H$ resonances. Nor does this nonpolarizable histidine possess a normal p$K_a$: values range only from 4.20 for carp to 4.32 for pike to 4.44 for rat. The $C_2H$ and $C_5H$ resonances of the histidine in this carp isoform split into doublets as the pH is lowered. The magnitude of this splitting depends on the magnetic field strength, temperature, and pH; however, the line intensities within each doublet are temperature-independent. Although the crystal structure of carp parvalbumin indicates that His-26 is exposed to solvent [Kretsinger, R. H., & Nockolds, C. E. (1973) *J. Biol. Chem. 248*, 3313–3326], we conclude that in solution this residue, in its unprotonated state, is part of the hydrophobic core of the protein. In contrast, His-48 in rat parvalbumin and His-106 in pike III parvalbumin show dramatic photo-CIDNP enhancements of their $C_2H$, $C_5H$, and $\beta$-$CH_2$ $^1$H NMR resonances. Combined with its nearly normal p$K_a$, 6.14, and exchange-broadened $C_2H$ resonance, the photo-CIDNP enhancement results for His-48 indicate that its microenvironment differs little from random-coil exposure, consistent with its presumed position on the solvent surface of helix C. However, the protonation behavior of His-106 in pike III suggests that its microenvironment is different from random-coil exposure. Not only is its p$K_a$ elevated (7.10) and $C_2H$ resonance minimally broadened, but its $C_5H$ resonance is also extremely sensitive to protonation/deprotonation of His-25. Because of the mutual sensitivity of the $C_5H$ resonances of His-25 and His-106 to the protonation/deprotonation of their imidazole rings, we suggest (i) that the protonated form of His-106 is involved in a H bond with a backbone C=O or side-chain –OH in the BC-linker region and (ii) that the protonated form of His-25(26) is expelled from the hydrophobic core. Each of these protonations causes a conformational change in the B-helix/F-helix region. In addition, photo-CIDNP studies of the p$I$ = 3.95 isoform of carp parvalbumin indicate that its single potentially enhanceable residue, Tyr-2, is either buried or involved in H-bond formation via its phenolic –OH group.

Few protein-bound protons have been such useful $^1$H NMR[1] spectroscopic probes of intrinsic tertiary structure as have the $C_2H$ and $C_5H$ imidazole-ring protons of histidine.[2] Not only are their resonances ordinarily observed as singlets in the relatively uncrowded aromatic region of the $^1$H NMR spectrum, but they are also extraordinarily sensitive to pH changes. These attributes, combined with the paucity of histidines in many proteins, facilitate the assignment of resonance pairs (i.e., $C_2H$ and $C_5H$) to specific residues in the amino acid sequence. Spectral perturbations of assigned histidine resonances can then be unequivocally attributed to discrete molecular perturbations in the folded protein (Markley, 1975a).

The microenvironments of individual histidines within a protein have most frequently been assessed by comparisons of their protonation parameters (e.g., p$K_a$, $^1H \rightarrow {}^2H$ exchange rates) with those of the free N-acetylated methyl ester or methylamide of histidine (Tanokura et al., 1978; Boschcov et al., 1983). In particular, variations in p$K_a$ have usually been ascribed to the nearness of the imidazole ring to charged, ionizable groups or its participation in H bonding, sluggish

† This work was supported by the Medical Research Council of Canada Group in Protein Structure and Function and the Alberta Heritage Foundation for Medical Research (equipment grant for the NT-300WB spectrometer and fellowship and research allowance to T.C.W.).

[1] Abbreviations: AB, helix A–loop–helix B region of parvalbumin (residues 7–34); CD, helix C–loop–helix D region of parvalbumin (residues 39–71); EF, helix E–loop–helix F region of parvalbumin (residues 78–108); ED, ethylenediamine; FMN, flavin mononucleotide (riboflavin phosphate); SDS, sodium dodecyl sulfate; $D_2O$, deuterium oxide; Tris, tris(hydroxymethyl)aminomethane; Pipes, 1,4-piperazinediethanesulfonic acid; DSS, sodium 4,4-dimethyl-4-silapentane-1-sulfonate; NMR, nuclear magnetic resonance; photo-CIDNP, photochemically induced dynamic nuclear polarization; NOE, nuclear Overhauser effect; UV, ultraviolet; FID, free induction decay.

[2] In accordance with nomenclature recommendations (IUPAC–IUB Joint Commission on Biochemical Nomenclature, 1985), we refer to the imidazole ring protons as $C_2H$ and $C_5H$ rather than $C_2H$ and $C_4H$ as has been done frequently in the past.

0006-2960/86/0425-1826$01.50/0 